Aalborg Universitet

AALBORG UNIVERSITY
DENMARK

Hyperoxia affects the lung tissue

A porcine histopathological and metabolite study using five hours of apneic oxygenation

Magnusdottir, Sigriður Olga; Maltesen, Raluca Georgiana; Banch, Lise Haugaard; Baandrup, Ulrik Thorngren; Valbjørn, Heidi Maria; Andreassen, Trygve ; Bathen, Tone Frost; Rasmussen, Bodil Steen; Kjærgaard, Benedict

Hyperoxia affects the lung tissue: A porcine histopathological and metabolite study using five hours of apneic oxygenation

Sigríður Olga Magnúsdóttir [a, b, *], Raluca Georgiana Maltesen [c], Lise Haugaard Banch [e],
Ulrik Thorngren Baandrup [e], Heidi Valbjørn [f], Trygve Andreassen [g], Tone Frost Bathen [g],
Bodil Steen Rasmussen [b, c], Benedict Kjærgaard [a, b, d]

[a] Biomedical Research Laboratory, Aalborg University Hospital, Aalborg, Denmark
[b] Department of Clinical Medicine, Aalborg University Hospital, Aalborg, Denmark
[c] Department of Anesthesia and Intensive Care, Aalborg University Hospital, Aalborg, Denmark
[d] Department of Cardiothoracic Surgery, Aalborg University Hospital, Aalborg, Denmark
[e] Center for Clinical Research and Pathology, Regional Hospital Nordjylland, Hjoerring, Denmark
[f] Department of Pathology, Aalborg University Hospital, Aalborg, Denmark
[g] Department of Circulation and Medical Imaging, MR Core Facility, NTNU − the Norwegian University of Science and Technology, Trondheim, Norway

ARTICLE INFO

ABSTRACT

Background: Oxygen is a liberally dosed medicine; however, too much oxygen can be harmful. In certain situations, treatment with high oxygen concentration is necessary, e.g. after cardiopulmonary resuscitation. The amount of oxygen and duration of hyperoxia causing pulmonary damage is not fully elucidated. The aim of this study was to investigate pathophysiological and metabolite changes in lung tissue during hyperoxia while the lungs were kept open under constant low pressure.
Methods: Seven pigs were exposed to 100% oxygen for five hours, using an apneic oxygenation technique with one long uninterrupted inspiration, while carbon dioxide was removed with an interventional lung assist. Arterial blood samples were collected every 30 minutes. Lung biopsies were obtained before and after hyperoxia. Microscopy and high-resolution magic angle spinning nuclear magnetic resonance spectroscopy were used to detect possible pathological and metabolite changes, respectively. Unsupervised multivariate analysis of variance and paired sample tests were performed. A two-tailed p-value $\leq$ 0.05 was considered significant.
Results: No significant changes in arterial pH, and partial pressure of carbon dioxide, and no clear histopathological changes were observed after hyperoxia. While blood glucose and lactate levels changed to a minor degree, their levels dropped significantly in the lung after hyperoxia ($p \leq 0.04$). Reduced levels of antioxidants ($p \leq 0.05$), tricarboxylic acid cycle and energy ($p \leq 0.04$) metabolites and increased levels of several amino acids ($p \leq 0.05$) were also detected.
Conclusion: Despite no histological changes, tissue metabolites were altered, indicating that exposure to hyperoxia affects lung tissue matrix on a molecular basis.

1. Introduction

Oxygen is one of the most widely used therapeutic agents in the world and in conditions with life threatening hypoxia it can be lifesaving. It is often liberally dosed, particularly in critically ill patients requiring mechanical ventilation, leading to supra-physiological partial pressures of oxygen (PaO_2) [1−3]. Growing evidence indicates that too much oxygen may be harmful [4−6]. The organs most affected by normobaric hyperoxia are the lungs and eyes [4,7−9]. Since the lungs are exposed directly to oxygen in

* Corresponding author. Biomedical Research Laboratory, Aalborg University Hospital, Stengade 12, 9000, Aalborg, Denmark.
E-mail addresses: s.magnusdottir@rn.dk (S.O. Magnúsdóttir), rm@rn.dk (R.G. Maltesen), lise.haugaard@rn.dk (L. Haugaard Banch), utb@rn.dk (U.T. Baandrup), h.valbjoern@rn.dk (H. Valbjørn), trygve.andreassen@ntnu.no (T. Andreassen), tone.f.bathen@ntnu.no (T.F. Bathen), bodil.steen.rasmussen@rn.dk (B. Steen Rasmussen), benedict.kjaergaard@rn.dk (B. Kjærgaard).

the alveoli and indirectly by the blood in the pulmonary vessels, hyperoxia may cause more damage to the lung tissue compared to other tissues. Exposure time, atmospheric pressure, and fraction of inspired oxygen (FiO_2) determine the cumulative oxygen amount leading to toxicity [6]. The severity of the hyperoxic lung tissue injury is directly proportional to the partial pressure of oxygen (PaO_2), particularly above 60 kPa or a FiO_2 approaching 1.0, and exposure time [4,6]. The pathological changes induced by hyperoxia are not specific and resemble pathological changes seen in other acute pulmonary diseases, such as the acute respiratory distress syndrome [10,11]. The earliest changes seen microscopically are capillary congestion, intra-alveolar hemorrhages, and interstitial and alveolar edema [12]. Infiltration of inflammatory cells from the blood to the lung tissue, such as lymphocytes, macrophages and plasma cells, as well as mild endothelial injury have also been reported [11]. These changes eventually lead to impaired gas exchange and multiorgan dysfunction [13].

Currently, the amount of oxygen causing pulmonary damage is still not fully elucidated. Numerous human and animal model studies have been performed with varying exposure time, FiO_2 and with or without mechanical ventilation [10,14—22]. Exposure of the lung tissue with an FiO_2 of 0.75—1.0 for 90 minutes has been reported to cause interstitial edema with subsequent intrusion of inflammatory and red blood cells into the alveoli, along with thickening of alveolar septa in Wistar rats [23]. In healthy humans, exposure to a FiO_2 of 0.95 elicited hyperoxia-induced alveolar capillary leak after 17 hours. These changes were reversible and disappeared within two weeks after the exposure [15]. Baboons exposed to 100% oxygen first showed signs of alveolar septal thickening after 80 hours of exposure [21], whereas in young Yorkshire pigs exposed to a FiO_2 above 0.80, capillary congestion and interstitial infiltration could be detected with light microscopy after 48 hours of exposure [24]. *In-vitro* research has demonstrated that human lung endothelial cells exposed to hyperoxia for 3—12 hours had enhanced nicotinamide adenine dinucleotide phosphate (NADPH) and nicotinamide adenine dinucleotide (NADH)-dependent reactive oxygen species (ROS) production [25]. In ovine lung endothelial cells exposed to hyperoxia for 30 minutes, free radicals were produced via the mitochondrial electron transport chain without the induction of cell death [26].

Ventilator treatment itself can cause damage to the lungs. The mechanisms involved are barotrauma, volutrauma and atelectrauma [27]. Barotrauma is due to high inflation pressure-mediated lung injury [28]. Volutrauma occurs because of overdistension-mediated lung injury [27]. Using low volume ventilation can also cause injury through multiple factors, such as opening and closing of lung units, impact on surfactant and regional hypoxia. These injuries are called atelectrauma [27]. It is therefore recommended to keep tidal volume low, peak pressure low and applying positive end expiratory pressure (PEEP) to reduce the risk of ventilator induced lung injury [29—31].

We hypothesize that hyperoxic-induced lung tissue injury affects the molecular balance and that these changes can be detected at an earlier stage compared to the characteristic histopathological changes. The application of apneic oxygenation enables the assessment of the effect of hyperoxia on lung tissue, minimizing interference from possible ventilator-induced injuries. During apneic oxygenation, pure oxygen is administered with low pressure to the cuffed endotracheal tube as one long uninterrupted inspiration, while carbon dioxide (CO_2) is removed with interventional lung assist (iLA). Hence, the aim of this study was to identify possible histopathological and molecular changes in lung tissue exposed to a very high oxygen tension. Due to the anatomical and immunological similarities between the porcine and human lung, pigs make an excellent model for human respiratory disease and pathologies [24,32]. Two lung biopsies were collected from seven pigs before induction of hyperoxia and after five hours of exposure to a FiO_2 of 1.0 and histopathological and metabolite analyses were performed.

2. Materials and methods

2.1. Animal care and anesthesia protocol

Seven 45 kg female Danish Landrace pigs were enrolled in this study after ethical approval by The Danish National Animal Ethics Committee (No. 2016-15-0201-00930).

The animals were allowed to acclimatize for six days before the experiments, with free access to water and food. Prior to the experimental procedure, overnight fasting was required. Anesthesia was induced with intramuscular injection of Zoletil®Vet, a mixture of ketamine (8.33 mg/mL) and tiletamine (8.33 mg/mL), benzodiazepine zolazepam (8.33 mg/mL), synthetic opioid butorphanol (1.67 mg/mL), and xylazin (8.33 mg/mL). The trachea was intubated (Portex tube, ID 6.5 mm, Smiths Medical, UK) and the lungs were mechanically ventilated (Dameca DREAM, Roedovre, Denmark) with tidal volume 6—8 mL/kg, FiO_2 0.23, inspiratory/expiratory ratio 1:2 and positive end-expiratory pressure 5 cm H_2O. Respiratory rate was adjusted to keep end-tidal carbon dioxide ($ETCO_2$) at 4.5—5.5 kPa. Anesthesia was maintained with continuous intravenous infusion of propofol (4 mg/kg/h) and fentanyl (5 µg/kg/h); the infusion rates were adjusted to maintain sufficient depth of anesthesia. Monitoring with electrocardiogram and peripheral oxygen saturation (SpO_2) was established. A bladder catheter with thermosensor (Degania Silicone Ltd. Degania Bet 15130, Israel) was inserted.

2.2. Experimental protocol

A catheter was inserted into the left external jugular vein for medicine and saline infusion, and another catheter was inserted into the right carotid artery for the measurement of arterial pressure and blood sampling for arterial blood gas analyses. Blood gases were analyzed using an automatic blood gas analyzer (ABL 800 flex, Radiometer, Bronshoej, Denmark).

Two lung biopsies were taken with a stapler (Endo GIA^{TM} Auto Suture^{TM}, Covidien, USA) from the left middle lung lobe, through a small thoracotomy, ensuring that the lung could be inflated afterwards.

A 17- and 19- french catheter (Novaport Vascular Access, Novalung, Germany) were inserted into the femoral artery and vein, respectively. These catheters were connected to an interventional lung assist device (iLA Membrane Ventilator, Novalung Gmbh, Germany) ensuring CO_2 removal from the circulation. The device was primed with isotonic saline and the extracorporeal circuit was opened. The blood flow in the extracorporeal circuit unit was monitored with an ultrasonic flow meter (NovaFlow s, Novalung GmbH), placed on the tube from the arterial catheter. Before cannulation 15.000 IE heparin was given for anticoagulation, and then 5.000 IE heparin was given every second hour to reduce the risk of clotting. The gas flow to the iLA was 100% oxygen at 10 L/min. throughout the whole experiment. Apneic oxygenation was established via tracheal gas insufflation through a catheter, connected to the orotracehal tube at one end and connected to a y-piece at the other end. The y-piece was connected to the oxygen supply and to a water manometer ensuring continuous pressure of 20 cm H_2O in the system (Fig. 1). The oxygen flow (1—3 L/min) was regulated to keep the water in the manometer bubbling [33,34].

After the preparation, when a steady state had been obtained, a set of baseline values were registered after which the mechanical

Fig. 1. Apneic oxygenation set-up. A thin tube was placed on the orotracheal tube. On the other end, the tube was connected to a y-piece (arrow). From the y-piece, a short tube was connected to a pressure regulator (container filled with water) and another short tube was connected to oxygen supply (oxygen supply not shown on picture).

ventilation was stopped and the iLA started. Arterial blood gas samples were taken every 30 minutes. A noradrenalin infusion was started (0.5 mg/h) if the systolic blood pressure dropped below 90 mmHg, to ensure a sufficient flow in the iLA. All pigs received noradrenaline infusion during the experimental period. The animals were kept on apneic oxygenation for 5 hours, two biopsies were then taken from the lung, using the same thoracotomy as before. The animals were then euthanized with an intravenous injection of pentobarbitone.

2.3. Sample preparation

Lung biopsy specimens were obtained for histological and metabolite examination, one for each examination, before and after the experiment. The samples taken before the experiment were defined as the baseline time point and the samples taken after the hyperoxia exposure were taken at 300 minutes (Table 1). The specimens for histopathology were initially immersion fixed in 4% buffered formalin and subsequently embedded in paraffin. A histopathological examination was performed on four μm tissue sections cut from the blocks. The samples were stained with HE (Haematoxylin-Eosin), Weigert stain, and Periodic acid−Schiff (PAS). This yielded six sections per pig, three from before oxygen treatment and three from after treatment. Furthermore, immunostains for T and B lymphocytes (CD3 and CD 20), epithelial markers (CK7), and endothelial markers (CD 34 and Factor VIII related antigen) were applied. Light microscopy was performed by an investigator unaware of which section was from before and after oxygen treatment. The other half of the lung biopsy specimens were flushed with saline and frozen in $-80\,°C$ freezer, for subsequent metabolomic experiments. High-resolution magic angle spinning (HR-MAS) nuclear magnetic resonance (NMR) spectra were recorded on a Bruker Avance III 600 MHz NMR spectrometer (Bruker Biospin GmbH, Rheinstetten, Germany) equipped with a triple resonance (^1H, ^{13}C, ^{31}P) HR-MAS probehead. Disposable Kel-F inserts with sodium formate solution in D_2O (25 mM, 5 μL) and freshly thawed tissue samples (9−16 mg), were placed in 4 mm zirconia MAS rotors. The rotors were spun at 5.000 Hz at $5\,°C$ during recordings. One-dimensional Carr-Purcell-Meiboom-Gill (CPMG) spectra were recorded with 72k data points, 256 scans, 20 ppm spectral width and a total echo time of 77 m s. Water pre-saturation (25 Hz) was applied during the relaxation delay (4 s). The CPMG NMR experiment is inherently non-quantitative, meaning that the individual metabolite signals are attenuated differently by the T2 filter, according to their transverse relaxation constants. In addition, the longitudinal relaxation (T1) for some nuclei will be too slow for complete relaxation during the combined acquisition time and relaxation delay, including the signal from the formate. However, given the presumption that relaxation properties are similar for all samples in the cohort, CPMG is useful for determining relative differences of metabolite levels.

2.4. Data analysis

CPMG spectra were manually phased and baseline corrected, calibrated to the alanine doublet at 1.48 ppm in TopSpin 3.1 (Bruker BioSpin, Rheinstetten, Germany) and reduced to integrals of 0.001 ppm bin width, excluding the water region (4.5−5.1 ppm) in AMIX (Analysis of MIXtures v. 3.9.10, Bruker BioSpin, Karlsruhe, Germany). Data was exported to MATLAB (R2018a, MathWork) and was subsequently normalized (probabilistic quotient normalization) and mean centered.

Unsupervised principal component analysis (PCA) was carried out on processed spectra in PLS Toolbox 6.5 (Eigenvector Research, Wenatchee, WA, USA) to identify possible outliers and trends in the data. Data was visualized by plotting the scores of the first two principal components (PC1 and PC2). Metabolites were assigned based on our previous study [35] and the Human Metabolite Database [36], while relative quantification was determined using the integrals produced by the line shape peak fitting option in MNOVA (Mestrelab Research v.12) relative to the known formate concentration and tissue weight.

Table 1
Baseline values and average a-gas parameters throughout the experiments. Values representing measurements from before (baseline) and end exposure time (300 min) are marked to emphasize that tissue samples collected at these time points were used for the histopathological and metabolomics experiments. Significance was calculated by means of repeated measurements analysis of variance (p-value time) and paired *t*-test calculated on samples collected before (baseline) and at the end of the exposure period (300 min) (p-value Baseline vs. 300 min). A 2-tailed p-value ≤ 0.05 was considered statistically significant.

		Baseline	0 min	30 min	60 min	90 min	120 min	150 min	180 min	210 min	240 min	270 min	300 min	p-value (time)	p-value (Baseline vs. 300 min)
pH	Mean	7.45	7.44	7.36	7.35	7.34	7.32	7.31	7.30	7.30	7.29	7.28	7.27	0.01	0.03
	SD	0.03	0.07	0.12	0.12	0.12	0.09	0.08	0.07	0.09	0.08	0.07	0.07		
PCO_2 (kPa)	Mean	5.35	5.34	6.17	6.13	6.43	6.46	6.61	6.47	6.62	6.70	6.68	6.86	0.89	0.15
	SD	0.5	0.9	1.9	1.9	2.1	1.9	1.9	1.5	1.9	1.9	1.6	1.8		
PO_2 (kPa)	Mean	22.1	51.6	53.0	59.1	59.9	62.0	63.6	61.8	59.6	62.3	60.2	58.4	0.006	0.003
	SD	13.1	16.4	18.8	13.4	16.6	14.4	16.0	15.5	14.8	16.1	13.9	14.4		
Lactate (mM)	Mean	1.1	1.2	1.5	1.6	1.6	1.8	1.8	1.7	1.5	1.4	1.3	1.2	0.81	0.68
	SD	0.2	0.6	0.6	0.4	0.5	0.7	0.6	0.6	0.6	0.6	0.6	0.5		
Glucose (mM)	Mean	6.2	5.7	6.5	6.2	6.4	6.2	6.2	5.3	5.1	4.9	4.8	4.7	0.43	0.055
	SD	2.3	2.4	3.4	1.9	2.3	2.0	1.9	2.1	2.1	1.9	1.6	1.7		

The statistical analysis was performed in the IBM®SPSS Statistics software (v. 25, SPSS Inc., Armonk, NY, USA). To be able to determine differences between paired samples collected before and after the exposure, we first employed a Shapiro-Wilk test to verify if the data followed a normal distribution. Accordingly, a paired *t*-test or its nonparametric equivalent Mann-Whitney-Wilcoxon rank test was applied. A calculated two-tailed p-value of less than or equal to 0.05 was considered statistically significant. Data was summarized using mean and standard deviation (SD), while scatter plots were used for visualization purposes.
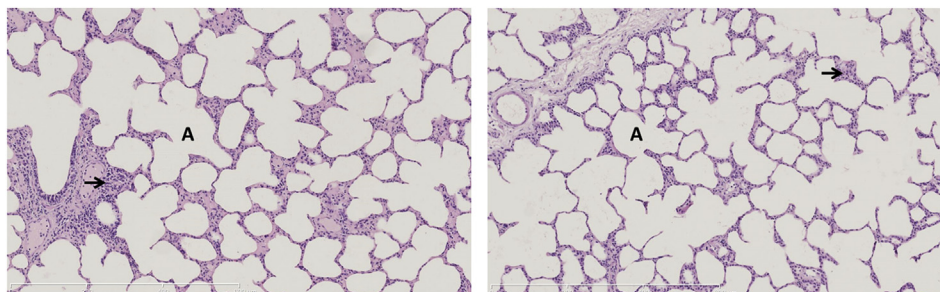
3. Results

One pig had to be excluded after three hours of hyperoxia due to hemodynamic instability; hence, six pigs were included in this study, (weight; mean $\pm$ SD, 45.6 $\pm$ 7.9 kg).

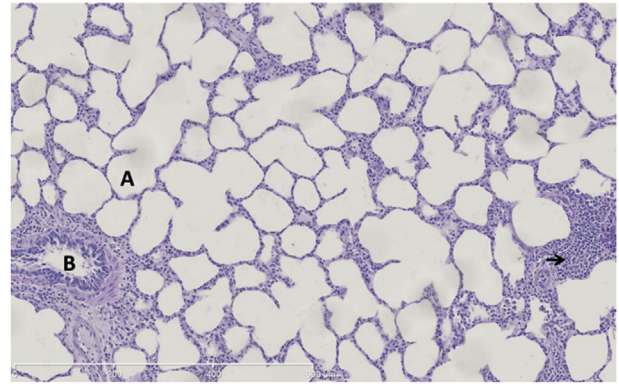### 3.1. Blood gas measurements

Arterial blood gas measurements performed at different time points before and during the exposure confirmed the presence of hyperoxia (Table 1). At the end of the experiment, pH levels dropped slightly in all animals. The partial pressure of carbon dioxide presented minor increases across the experimental period; however, these changes were within the normal range. As expected, the partial pressure of oxygen was above physiological values during exposure to hyperoxia, with mean values between 52 and 64 kPa, due to the high FiO$_2$ received. The increase in PaO$_2$ was pronounced already from the first arterial blood gas drawn after initiating the iLA and remained above 50 kPa throughout the experiment. Lastly, while arterial blood glucose levels were slightly decreased after 300 minutes of hyperoxia, lactate levels remained mainly unchanged, indicating successful circulation in the pigs during the experimental procedure.

3.2. Lung histological characterization

Lung tissue biopsies were obtained before and after the exposure. Paired samples were evaluated on size, pleural, interstitial and parenchymatous morphology. Large inter- and intra-individual differences were observed in the histopathological sections across the animals, with no visible characteristic changes related to the oxygen treatment received (Fig. 2). No hyaline membranes were detected (Fig. 3). Elastic fibers, T- or B-lymphocytes and epithelial and endothelial cells did not differ between samples taken before and after the oxygen exposure, indicating that vascular permeability was not increased during the five hours of hyperoxia.


Fig. 3. Lung histological changes after five-hour hyperoxia. Pig no. 4, PAS staining, after hyperoxia. No hyaline membranes are seen. Morphology does not differ from Fig. 1. Normal alveoli (A), local lymphocytic infiltration (arrow) and bronchiole (B).

3.3. Lung metabolite profiles of hyperoxia

To analyze the metabolic response to hyperoxia, unsupervised PCA was performed on processed spectra. Samples clustered according to the experimental conditions (Fig. 4); with tissue samples collected before and after hyperoxia along the positive principal component 1 (PC1) axis, and tissue samples affected by hyperoxia along the negative PC1. Several metabolites were found to be different between the paired samples (Table 2). The most relevant
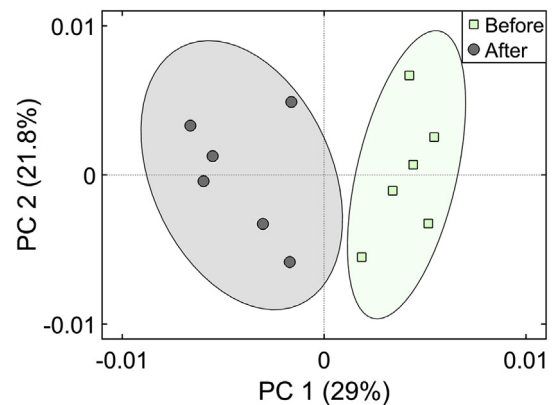
Fig. 4. Lung metabolic profile changes as a consequence of hyperoxia. Principal component analysis performed on processed spectra revealed sample clustering along first principal component (PC1) according to the time of sample collection; before (green, along + PC1) and after hyperoxia (gray, along -PC1). (For interpretation of the references to colour in this figure legend, the reader is referred to the Web version of this article.)

Fig. 2. Lung histological changes during five-hour hyperoxia. Left: Pig no. 1, HE staining, before hyperoxia. Normal alveoli (A), local lymphocytic infiltration (arrow). **Right**: Pig no. 1, HE staining, after hyperoxia. Normal alveoli (A), local lymphocytic infiltration (arrow). Morphology does not differ between the two figures.

Table 2
Metabolites that changed during the five hours hyperoxia treatment. Paired *t*-test or its non-parametric equivalent Wilcoxon signed rank test was used to detect possible differences between pair samples. Data is presented as mean and standard deviations (SD). A 2-tailed p-value ≤ 0.05 was considered statistically significant.

| Metabolites	Before (pmol/mg)		After (pmol/mg)		Pair t-/Wilcoxon Signed Ranks Test Sig. (2-tailed)
	Mean	SD	Mean	SD	
Nicotinate	680	169	415	110	0.02
Adenosine	350	60	282	63	0.03
Inosine	83	8	72	13	0.06
Hypoxanthine	527	60	652	158	0.03
Histidine	22	27	263	157	0.03
Uracil	60	46	93	57	0.13
Phenylalanine	158	62	337	216	0.11
Tryptothan	302	49	522	226	0.07
Tyrosine	136	36	236	149	0.07
Fumarate	30	8	12	7	0.004
ATP	279	124	164	101	0.13
AMP & IMP	272	49	214	65	0.01
Fatty acyl chain	438	187	705	290	0.08
a-Glucose	1512	374	1269	439	0.04
Glycerophosphocholine	797	189	634	186	0.01
Phosphatidyl choline	1643	364	1353	454	0.017
Lactate	6856	766	4792	1220	0.03
Myo-inositol	6324	802	5248	1287	0.03
Creatinine	1678	302	1353	278	0.001
Creatine	941	244	797	225	0.04
Glycine	9844	1333	8823	2419	0.23
Taurine	8298	1897	7025	2419	0.07
Sphingomyelin and Choline	2308	304	1769	413	0.02
Trimetylamine-N-oxide	5196	625	4492	1039	0.12
2-ketoglutarate	631	141	488	125	0.02
Aspartic acid	289	61	365	107	0.05
Glutathione	842	140	664	198	0.004
Citrate	419	99	261	35	0.02
Succinate	639	58	566	108	0.04
Glutamate	5925	1163	4567	1121	0.005
Glutamine	4340	616	3520	730	0.002
Acetate	338	65	416	82	0.03
Proline & Arginine	725	149	952	132	0.07
Alanine	1405	217	2337	411	0.002
Valine	306	31	495	171	0.03
Isoleucine	180	24	219	50	0.20
Leucine	330	44	465	91	0.04

metabolites are visualized in Fig. 5. Tissue glucose and lactate levels were reduced at the end of the experimental period, indicating deranged glycolysis with a subsequent effect on the organism's energy status, including ATP, adenosine monophosphate (AMP) and inosine monophosphate (IMP) (Fig. 5). In line with these findings, metabolites involved in the tricarboxylic acid (TCA) cycle including citrate, succinate, fumarate, and 2-ketoglutarate were also decreased. The oxidant and antioxidant metabolites hypoxanthine, uracil, uridine, adenine, inosine, aspartic acid, glutathione, and taurine were also found to be altered, indicating an increase in oxidative stress due to imbalance in the oxidant-antioxidant status following hyperoxia. In addition, the amino acids alanine, phenylalanine, valine, isoleucine and leucine, known to be involved in protein biosynthesis and/or degradation, were altered, while the phospholipids glycerophosphocholine, phosphatidylcholine, and sphingomyelin and choline, involved in cell membrane functions and surfactant synthesis, were decreased at the end of the experimental period (Fig. 5).

4. Discussion

To our knowledge, this is the first study investigating lung metabolite profiles of hyperoxia. This study demonstrates that despite the relatively unchanged lung histology after a five-hour exposure to hyperoxia, there were clear changes in the small metabolite levels. The general picture that emerges from our metabolomics approach is one of energy depletion, with decreased levels of glucose, ATP, AMP and IMP, suppressed TCA cycle, and increased production of ROS. Although the study investigates changes in a pig model, the findings can improve understanding of the biochemical and molecular alterations the lungs undergo during hyperoxic conditions, an event often encountered at intensive care units across the world. Metabolites are the end products of gene, transcript, and protein regulation, and are strongly influenced by environmental changes such as disease progression [35,37] and treatment administered [38,39]. Therefore, changes in their levels should reflect an overall molecular window of events occurring during hyperoxia. Previous studies have shown that the combination of increased ROS production together with the lack of cellular energy ultimately compromises the organism's antioxidant defense mechanism [40,41].

We did not induce hypoxia in our research as the method we used (apneic oxygenation) cannot be done with other gasses than oxygen [33]. However, by comparing the literature describing metabolomics studies performed on hypoxic human and animal models with our hyperoxia result, we have found that several metabolite changes were quite contrary, strengthening our findings. For example, our results show that hyperoxia is characterized by energy depletion, imbalance in the oxidant-antioxidant defense, and cell membrane and surfactant dysfunction. During hypoxia however, Heerlein and co-workers have found a reduced energy demand due to a decreased activity in ATP-consuming pathways [42]. Secondly, the levels of glutamate and glutathione were found diminishing after 5 hours of hyperoxia whereas they increased
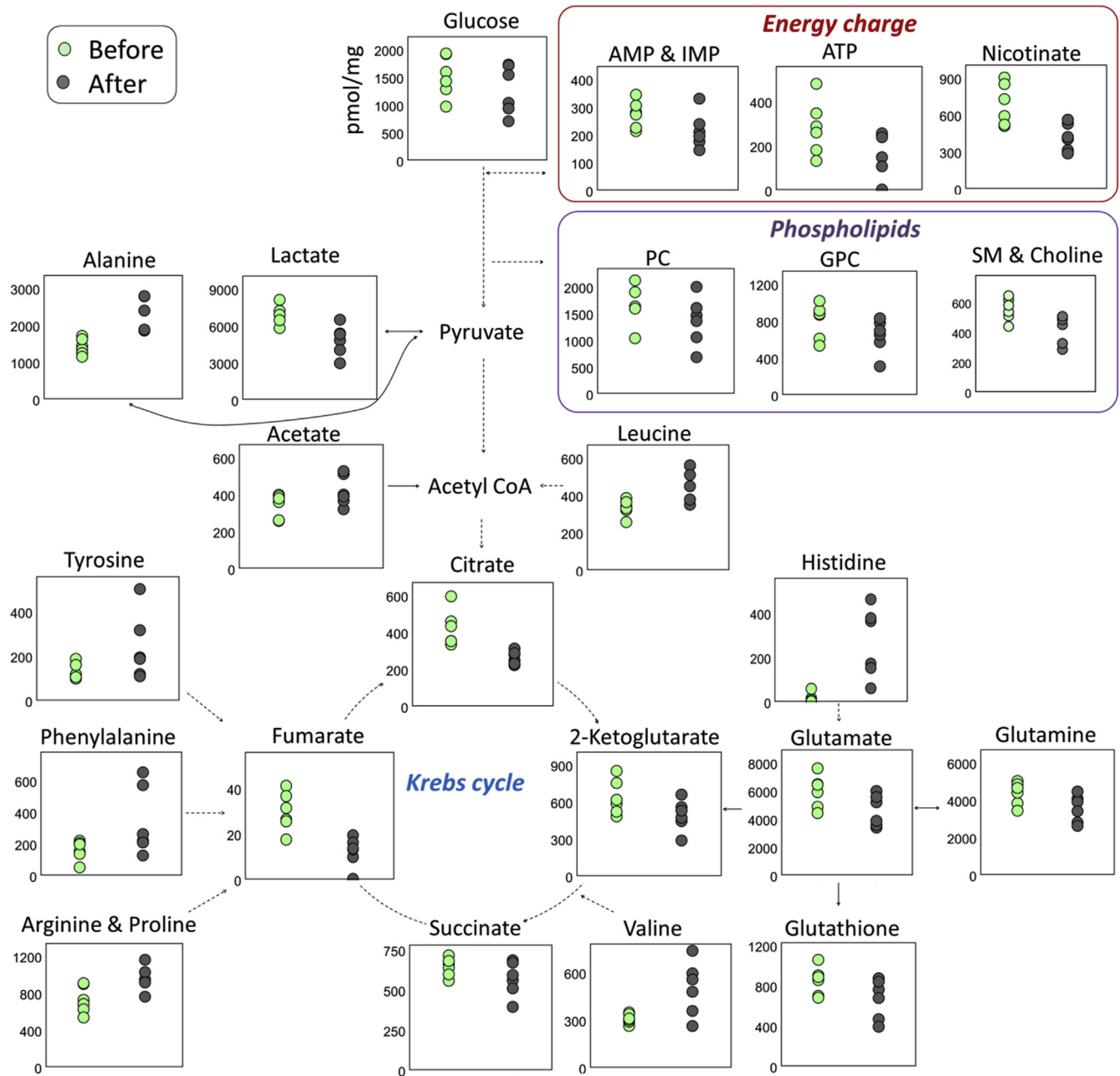
Fig. 5. Simplified pathways showing the metabolic hallmark of hyperoxia. Only identified and quantified metabolites are visualized. Abbreviation: ATP, adenosine triphosphate; AMP & IMP, adenosine monophosphate and inosine monophosphate; PC, phosphocholine; GPC, glycerophosphocholine; SM, sphingomyelin.

during hypoxia [43,44]. Moreover, in our study, tricarboxylic acid cycle (TCA) intermediates were found reduced while their levels increased in patients suffering from hypoxemia [43]. Lastly, hypoxanthine and histidine have been found reduced in patients suffering from hypoxemia [35]. In contrast, in our hyperoxia study, these metabolites were found elevated after 5 hours exposure of oxygen. Altogether, the contrasts in these metabolites levels indicate that the presence or lack of oxygen, as is the case of hyperoxia and hypoxia, respectively, influences same metabolite pathways but with opposing effect on metabolite levels.

4.1. Arterial blood gas changes during hyperoxia

Arterial blood gas measurements showed pronounced hyperoxia already from the first measurement after the apneic oxygenation was initiated (Table 1). The partial pressure of carbon dioxide increased during the experimental period and the pH levels dropped accordingly. Even though these changes were within normal ranges, they might have been avoided by increasing the sweep gas flow up to 15 L/min, which is the maximum recommended gas flow for the iLA device [45].

4.2. Lung tissue histological changes during hyperoxia

Healthy humans exposed to a FiO_2 of 0.95 at normobaric atmospheric pressure will have a latent period of 4–22 hours before experiencing any symptoms [15]. This latent period is generally accepted as clinically safe for hyperoxia treatment [46]. The first

histological findings after normobaric hyperoxia can be identified after 12−24 hours of exposure, the main findings being capillary congestion and interstitial and intra-alveolar edema [11]. This is consistent with our results from the lung tissue histopathology, where changes related to hyperoxia could not be detected, not even the appearance of a hyaline membrane, which is one of the hallmarks of the acute phase of pulmonary injury. Despite these negative results in the levels of inflammatory cells or the epithelial and endothelial cells, *in-vitro* studies performed on ovine pulmonary artery endothelial cells have shown that within 30 minutes of 100% oxygen exposure there is already increased production of superoxide anions and other radicals [26]. Parinandi and co-workers [25] found increased formation of H_2O_2 in human pulmonary artery endothelial cells exposed to 100% oxygen for 3 hours.

4.3. Lung metabolite profile of hyperoxia

Glucose is the most important metabolite in glycolysis, involved in the synthesis of ATP and NADH for cellular energy. In this study, glucose levels decreased both in blood and lung tissue samples. Our results confirm previous findings conducted on mouse lung tissue, where glycolytic activity was reduced [40]. The energy metabolites ATP, AMP and IMP were also decreased following hyperoxia, indicating an overall derangement of energy production in the lung tissue.

Imbalance in the levels of oxidants and antioxidants is thought to be one the key players in the pathogenesis of hyperoxic injuries. Since TCA can regulate the production and decomposition of antioxidants [47,48], it is interesting to observe that citrate, fumarate, succinate, and 2-ketoglutaric acid were decreased following the 5 hour period of hyperoxia. Chambellans and Lemires demonstrated that the cell's immediate response to hyperoxia is downregulating the antioxidant defenses resulting in protective cell cycle arrest to minimize the effects of hyperoxia [49,50], which is in line with our findings. An overall reduction was observed in the levels of the antioxidants nicotinate, inosine, and adenosine, and of the detoxification metabolite glutathione, the most abundant antioxidants present in cells [48], indicating increased consumption of antioxidants, increased production of ROS, or both. These findings have been previously confirmed in studies conducted on human and ovine pulmonary endothelial cells [25,26]. The precursors of glutathione, glutamine and glutamate, were also found to be decreased.

The levels of several amino acids were increased at the end of the hyperoxic period, possibly indicating augmented proteolysis, as suggested previously by Oury and co-workers [20] caused by the severe energy depletion occurring during hyperoxia [40].

Lastly, the lung tissue levels of choline and sphingomyelin, glycerophosphocholine, and phosphatidyl choline were lower after hyperoxia. These metabolites are known to be the main components of the pulmonary surfactants [51] and act as signaling molecules embedded in the cellular membrane [52], hence, our results possibly indicate dysfunctionality in either surfactant production, cell membrane integrity, or both.

4.4. Strength and limitations

The application of both histopathological and NMR studies to estimate the effect of hyperoxia on lung tissue is new and to our knowledge has not been attempted before. The interaction of oxygen with other pathological conditions cannot be evaluated without better knowledge of the injuries caused by oxygen alone. By using an apneic oxygenation technique during the experiments, any effect of the respirator treatment on the development of lung tissue damages could be minimized, hence, the changes observed are indeed caused by hyperoxia. Each pig served as its own control, minimizing the possible individual variation that can add confounding to the data. However, several practical limitations must be acknowledged. Although our study is the first of its kind published to date, sample size is small and the pigs used were young and healthy, whereas patients exposed to hyperoxia are critically ill and of varying ages. Furthermore, we did not have a set of blood samples to investigate metabolite changes as a consequence of hyperoxia. This information would have helped characterize the effect of hyperoxia on the whole metabolome. Additional studies are needed to investigate the whole body response to this stress factor. Increasing evidence shows that liberal oxygen therapy increases mortality in acutely ill adult [53]. With liberal oxygen therapy, the lungs are exposed to high concentrations of oxygen, which increases the risk of acute lung injury. This present porcine study visualizes significant metabolic changes in the lung tissues following exposure to 100% oxygen. In the clinical settings, lung biopsies are not possible; however, the results are important as no specific biomarkers for lung tissue injury exits. New studies using bronchoalveolar lavage and exhaled breath condensate will be needed to confirm the results in acutely ill patients.

5. Conclusion

Despite no histopathological changes being detected in the lung tissue after a period of five hours of hyperoxia, significant changes were observed in the levels of lung tissue metabolites. Hyperoxia is characterized by energy depletion, imbalance in the oxidant-antioxidant defense, possible proteolysis, and cell membrane and surfactant dysfunction. These results clearly indicate that providing FiO_2 of 1.0, and hence a high PaO_2, affects the lung tissue. Thus, this study emphasizes the need for further metabolite studies in critically ill patients. If the same metabolite pattern can be recognized, it might call for changes in targeting FiO_2, and thereby PaO_2, in order to minimize the risk of oxygens adverse effects.

Author contribution

B.S.R. and B.K. came up with the main research idea and supervised the project. S.O.M. and B.K executed the surgeries together, collected biopsies, and performed blood gas analyses. H.V. prepared the histopathological samples. L.H.B. and U.B. examined the histopathological samples. T.A. and T.F.B. prepared and performed the NMR experiments. R.G.M processed and performed data analysis. R.G.M. and S.O.M. interpreted the results. S.O.M. wrote the first draft of the paper. All authors assisted in drafting the manuscript and approved the final document.

Conflicts of interest

The authors declare no conflict of interest.

Regional Health Authority.

References

[1] de Jonge E, Peelen L, Keijzers PJ, Joore H, de Lange D, van der Voort PH, et al. Association between administered oxygen, arterial partial oxygen pressure and mortality in mechanically ventilated intensive care unit patients. Crit Care 2008;12:R156. https://doi.org/10.1186/cc7150.

[2] Suzuki S, Eastwood GM, Peck L, Glassford NJ, Bellomo R. Current oxygen management in mechanically ventilated patients: a prospective observational cohort study. J Crit Care 2013;28:647–54. https://doi.org/10.1016/j.jcrc.2013.03.010.

[3] Llitjos J-F, Mira J-P, Duranteau J, Cariou A. Hyperoxia toxicity after cardiac arrest: what is the evidence? Ann Intensive Care 2016;6. https://doi.org/10.1186/s13613-016-0126-8.

[4] Kallet RH, Matthay MA. Hyperoxic acute lung injury. Respir Care 2013;58:123–41. https://doi.org/10.4187/respcare.01963.

[5] Jackson RM. Pulmonary oxygen toxicity. Chest 1985;88:900–5. https://doi.org/10.1378/chest.88.6.900.

[6] Mach WJ, Thimmesch AR, Pierce JT, Pierce JD. Consequences of hyperoxia and the toxicity of oxygen in the lung. Nurs Res Pract 2011. https://doi.org/10.1155/2011/260482.

[7] Crapo JD. Morphologic changes in pulmonary oxygen toxicity. Annu Rev Physiol 1986;48:721–31. https://doi.org/10.1146/annurev.ph.48.030186.003445.

[8] Guaiquil VH, Hewing NJ, Chiang MF, Rosenblatt MI, Chan RVP, Blobel CP. A murine model for retinopathy of prematurity identifies endothelial cell proliferation as a potential mechanism for plus Disease Increased proliferation of vascular cells in plus disease. Investig Ophthalmol Vis Sci 2013;54:5294–302. https://doi.org/10.1167/iovs.12-11492.

[9] Mohamed I, Elremaly W, Rouleau T, Lavoie J-C. Oxygen and parenteral nutrition two main oxidants for extremely preterm infants: "It all adds up. J Neonatal Perinat Med 2015;8:189–97. https://doi.org/10.3233/NPM-15814091.

[10] Davis JM, Penney DP, Notter RH, Metlay L, Dickerson B, Shapiro DL. Lung injury in the neonatal piglet caused by hyperoxia and mechanical ventilation. J Appl Physiol 1989;67:1007–12. https://doi.org/10.1152/jappl.1989.67.3.1007.

[11] Castro CY. ARDS and diffuse alveolar damage: a pathologist's perspective. Semin Thorac Cardiovasc Surg 2006;18:13–9. https://doi.org/10.1053/j.semtcvs.2006.02.001.

[12] Tomashefski JF. Pulmonary pathology of acute respiratory distress syndrome. Clin Chest Med 2000;21:435–66.

[13] Perl M, Lomas-Neira J, Venet F, Chung C-S, Ayala A. Pathogenesis of indirect (secondary) acute lung injury. Expert Rev Respir Med 2011;5:115–26. https://doi.org/10.1586/ers.10.92.

[14] Caldwell PR, Lee WL, Schildkraut HS, Archibald ER. Changes in lung volume, diffusing capacity, and blood gases in men breathing oxygen. J Appl Physiol 1966;21:1477–83. https://doi.org/10.1152/jappl.1966.21.5.1477.

[15] Davis WB, Rennard SI, Bitterman PB, Crystal RG. Pulmonary oxygen toxicity. N Engl J Med 1983;309:878–83. https://doi.org/10.1056/NEJM198310133091502.

[16] Kapanci Y, Tosco R, Eggermann J, Gould VE. Oxygen pneumonitis in man: light- and electron-microscopic morphometric studies. Chest 1972;62:162–9. https://doi.org/10.1378/chest.62.2.162.

[17] Yam J, Roberts RJ. Oxygen-induced lung injury in the newborn piglet. Early Hum Dev 1980;4:411–24.

[18] Barry BE, Crapo JD. Patterns of accumulation of platelets and neutrophils in rat lungs during exposure to 100% and 85% oxygen. Am Rev Respir Dis 1985;132:548–55. https://doi.org/10.1164/arrd.1985.132.3.548.

[19] Crapo JD, Barry BE, Foscue HA, Shelburne J. Structural and biochemical changes in rat lungs occurring during exposures to lethal and adaptive doses of oxygen. Am Rev Respir Dis 1980;122:123–43. https://doi.org/10.1164/arrd.1980.122.1.123.

[20] Oury TD, Schaefer LM, Fattman CL, Choi A, Weck KE, Watkins SC. Depletion of pulmonary EC-SOD after exposure to hyperoxia. Am J Physiol Lung Cell Mol Physiol 2002;283:L777–84. https://doi.org/10.1152/ajplung.00011.2002.

[21] Fracica PJ, Knapp MJ, Piantadosi CA, Takeda K, Fulkerson WJ, Coleman RE, et al. Responses of baboons to prolonged hyperoxia: physiology and qualitative pathology. J Appl Physiol 1991;71:2352–62. https://doi.org/10.1152/jappl.1991.71.6.2352.

[22] Helmerhorst HJF, Schouten LRA, Wagenaar GTM, Juffermans NP, JJTH Roelofs, Schultz MJ, et al. Hyperoxia provokes a time- and dose-dependent inflammatory response in mechanically ventilated mice, irrespective of tidal volumes. Intensive Care Med Exp 2017;5. https://doi.org/10.1186/s40635-017-0142-5.

[23] Nagato A, Silva FL, Silva AR, Bezerra FS, Oliveira ML, Belló-Klein A, et al. Hyperoxia-induced lung injury is dose dependent in wistar rats. Exp Lung Res 2009;35:713–28. https://doi.org/10.3109/01902140902853184.

[24] Gushima Y, Ichikado K, Suga M, Okamoto T, Iyonaga K, Sato K, et al. Expression of matrix metalloproteinases in pigs with hyperoxia-induced acute lung injury. Eur Respir J 2001;18:827–37.

[25] Parinandi NL, Kleinberg MA, Usatyuk PV, Cummings RJ, Pennathur A, Cardounel AJ, et al. Hyperoxia-induced NAD(P)H oxidase activation and

[26] regulation by MAP kinases in human lung endothelial cells. Am J Physiol Lung Cell Mol Physiol 2003;284:L26–38. https://doi.org/10.1152/ajplung.00123.2002.

[26] Sanders SP, Zweier JL, Kuppusamy P, Harrison SJ, Bassett DJ, Gabrielson EW, et al. Hyperoxic sheep pulmonary microvascular endothelial cells generate free radicals via mitochondrial electron transport. J Clin Investig 1993;91:46–52. https://doi.org/10.1172/JCI116198.

[27] Beitler JR, Malhotra A, Thompson BT. Ventilator-induced lung injury. Clin Chest Med 2016;37:633–46. https://doi.org/10.1016/j.ccm.2016.07.004.

[28] Slutsky AS, Ranieri VM. Ventilator-induced lung injury. N Engl J Med 2013;369:2126–36. https://doi.org/10.1056/NEJMra1208707.

[29] Fan E, Brodie D, Slutsky AS. Acute respiratory distress syndrome: advances in diagnosis and treatment. J Am Med Assoc 2018;319:698–710. https://doi.org/10.1001/jama.2017.21907.

[30] Fan E, Del Sorbo L, Goligher EC, Hodgson CL, Munshi L, Walkey AJ, et al. An official American thoracic society/european society of intensive care medicine/society of critical care medicine clinical practice guideline: mechanical ventilation in adult patients with acute respiratory distress syndrome. Am J Respir Crit Care Med 2017;195:1253–63. https://doi.org/10.1164/rccm.201703-0548ST.

[31] Claesson J, Freundlich M, Gunnarsson I, Laake JH, Vandvik PO, Varpula T, et al. Scandinavian clinical practice guideline on mechanical ventilation in adults with the acute respiratory distress syndrome. Acta Anaesthesiol Scand 2015;59:286–97. https://doi.org/10.1111/aas.12449.

[32] Judge EP, Hughes JML, Egan JJ, Maguire M, Molloy EL, O'Dea S. Anatomy and bronchoscopy of the porcine lung. A model for translational respiratory medicine. Am J Respir Cell Mol Biol 2014;51:334–43. https://doi.org/10.1165/rcmb.2013-0453TR.

[33] Nielsen ND, Andersen G, Kjaergaard B, Staerkind ME, Larsson A. Alveolar accumulation/concentration of nitrogen during apneic oxygenation with arteriovenous carbon dioxide removal. ASAIO J Am Soc Artif Intern Organs 1992 2010;56:30–4. https://doi.org/10.1097/MAT.0b013e3181c4e935.

[34] Nielsen ND, Kjærgaard B, Koefoed-Nielsen J, Steensen CO, Larsson A. Apneic oxygenation combined with extracorporeal arteriovenous carbon dioxide removal provides sufficient gas exchange in experimental lung injury. ASAIO J 2008;54:401. https://doi.org/10.1097/MAT.0b013e31817e2b5f.

[35] Maltesen RG, Hanifa MA, Kucheryavskiy S, Pedersen S, Kristensen SR, Rasmussen BS, et al. Predictive biomarkers and metabolic hallmark of post-operative hypoxaemia. Metabolomics 2016;12:87. https://doi.org/10.1007/s11306-016-1018-5.

[36] Wishart DS, Jewison T, Guo AC, Wilson M, Knox C, Liu Y, et al. HMDB 3.0—the human metabolome Database in 2013. Nucleic Acids Res 2013;41:D801–7. https://doi.org/10.1093/nar/gks1065.

[37] Maltesen RG, Rasmussen BS, Pedersen S, Hanifa MA, Kucheryavskiy S, Kristensen SR, et al. Metabotyping patients' journeys reveals early predisposition to lung injury after cardiac surgery. Sci Rep 2017;7. https://doi.org/10.1038/srep40275.

[38] Buggeskov KB, Maltesen RG, Rasmussen BS, Hanifa MA, Lund MAV, Wimmer R, et al. Lung protection strategies during cardiopulmonary bypass affect the composition of blood electrolytes and metabolites—a randomized controlled trial. J Clin Med 2018;7. https://doi.org/10.3390/jcm7110462.

[39] Maltesen RG, Buggeskov KB, Andersen CB, Plovsing R, Wimmer R, Ravn HB, et al. Lung protection strategies during cardiopulmonary bypass affect the composition of bronchoalveolar fluid and lung tissue in cardiac surgery patients. Metabolites 2018;8:54. https://doi.org/10.3390/metabo8040054.

[40] Das KC. Hyperoxia decreases glycolytic capacity, glycolytic reserve and oxidative phosphorylation in MLE-12 cells and inhibits complex I and II function, but not complex IV in isolated mouse lung mitochondria. PLoS One 2013;8. https://doi.org/10.1371/journal.pone.0073358.

[41] Nita M, Grzybowski A. The role of the reactive oxygen species and oxidative stress in the pathomechanism of the age-related ocular diseases and other pathologies of the anterior and posterior eye segments in adults. Oxid Med Cell Longev 2016. https://doi.org/10.1155/2016/3164734.

[42] Heerlein K, Schulze A, Hotz L, Bärtsch P, Mairbäurl H. Hypoxia decreases cellular ATP demand and inhibits mitochondrial respiration of A549 cells. Am J Respir Cell Mol Biol 2005;32:44–51. https://doi.org/10.1165/rcmb.2004-0202OC.

[43] Stringer KA, Serkova NJ, Karnovsky A, Guire K, Paine R, Standiford TJ. Metabolic consequences of sepsis-induced acute lung injury revealed by plasma 1H-nuclear magnetic resonance quantitative metabolomics and computational analysis. Am J Physiol Lung Cell Mol Physiol 2010;300. https://doi.org/10.1152/ajplung.00231.2010. L4–11.

[44] Viswan A, Singh C, Rai RK, Azim A, Sinha N, Baronia AK. Metabolomics based predictive biomarker model of ARDS: a systemic measure of clinical hypoxemia. PLoS One 2017;12:e0187545. https://doi.org/10.1371/journal.pone.0187545.

[45] Fischer S. The Novalung(R) iLA membrane ventilator: technical aspects n.d.

[46] Bitterman H. Bench-to-bedside review: oxygen as a drug. Crit Care 2009;13:205. https://doi.org/10.1186/cc7151.

[47] Liu J, Litt L, Segal MR, Kelly MJS, Pelton JG, Kim M. Metabolomics of oxidative stress in recent studies of endogenous and exogenously administered intermediate metabolites. Int J Mol Sci 2011;12:6469–501. https://doi.org/10.3390/ijms12106469.

[48] Jana SK, Dutta M, Joshi M, Srivastava S, Chakravarty B, Chaudhury K. 1H NMR based targeted metabolite profiling for understanding the complex

relationship connecting oxidative stress with endometriosis. BioMed Res Int 2013;2013. https://doi.org/10.1155/2013/329058.

[49] Chambellan A, Cruickshank PJ, McKenzie P, Cannady SB, Szabo K, Comhair SAA, et al. Gene expression profile of human airway epithelium induced by hyperoxia in vivo. Am J Respir Cell Mol Biol 2006;35:424—35. https://doi.org/10.1165/rcmb.2005-0251OC.

[50] Lemire J, Milandu Y, Auger C, Bignucolo A, Appanna VP, Appanna VD. Histidine is a source of the antioxidant, α-ketoglutarate, in Pseudomonas fluorescens challenged by oxidative stress. FEMS Microbiol Lett 2010;309:170—7. https://doi.org/10.1111/j.1574-6968.2010.02034.x.

[51] Agassandian M, Mallampalli RK. Surfactant phospholipid metabolism. Biochim Biophys Acta 2013;1831:612—25. https://doi.org/10.1016/j.bbalip.2012.09.010.

[52] Ghidoni R, Caretti A, Signorelli P. Role of sphingolipids in the pathobiology of lung inflammation. Mediat Inflamm 2015;2015. https://doi.org/10.1155/2015/487508.

[53] Chu DK, Kim LH-Y, Young PJ, Zamiri N, Almenawer SA, Jaeschke R, et al. Mortality and morbidity in acutely ill adults treated with liberal versus conservative oxygen therapy (IOTA): a systematic review and meta-analysis. Lancet Lond Engl 2018;391:1693—705. https://doi.org/10.1016/S0140-6736(18)30479-3.